

# Joint processing of linguistic properties in brains and language models

Subba Reddy Oota<sup>1,2</sup>, Manish Gupta<sup>3</sup>, Mariya Toneva<sup>2</sup>

<sup>1</sup>Inria Bordeaux, France, <sup>2</sup>MPI for Software Systems, Saarbrücken, Germany, <sup>3</sup>Microsoft, India

subba-reddy.oota@inria.fr, gmanish@microsoft.com, mtoneva@mpi-sws.org

## Abstract

Language models have been shown to be very effective in predicting brain recordings of subjects experiencing complex language stimuli. For a deeper understanding of this alignment, it is important to understand the alignment between the detailed processing of linguistic information by the human brain versus language models. In NLP, linguistic probing tasks have revealed a hierarchy of information processing in neural language models that progresses from simple to complex with an increase in depth. On the other hand, in neuroscience, the strongest alignment with high-level language brain regions has consistently been observed in the middle layers. These findings leave an open question as to what linguistic information actually underlies the observed alignment between brains and language models. We investigate this question via a direct approach, in which we eliminate information related to specific linguistic properties in the language model representations and observe how this intervention affects the alignment with fMRI brain recordings obtained while participants listened to a story. We investigate a range of linguistic properties (surface, syntactic and semantic) and find that the elimination of each one results in a significant decrease in brain alignment across all layers of a language model. These findings provide direct evidence for the role of specific linguistic information in the alignment between brain and language models, and opens new avenues for mapping the joint information processing in both systems.

## 1 Introduction

Language models that have been pretrained for the next word prediction task using millions of text documents can significantly predict brain recordings of people comprehending language (Wehbe et al., 2014; Jain and Huth, 2018; Toneva and Wehbe, 2019; Caucheteux and King, 2020; Schrimpf et al.,

2021; Goldstein et al., 2022). Understanding the reasons behind the observed similarities between language comprehension in machines and brains can lead to more insight into both systems.

While such similarities have been observed at a coarse level, it is not yet clear whether and how the two systems align in their information processing pipeline. This pipeline has been studied separately in both systems. In natural language processing (NLP), researchers use probing tasks to uncover the parts of the model that encode specific linguistic properties (e.g. sentence length, tree depth, top constituents, tense, bigram shift, subject number, object number) (Adi et al., 2016; Hupkes et al., 2018; Conneau et al., 2018; Jawahar et al., 2019; Rogers et al., 2020). These techniques have revealed a hierarchy of information processing in multi-layered language models that progresses from simple to complex with increase in depth. In cognitive neuroscience, traditional experiments study the processing of specific linguistic properties by carefully controlling the experimental stimulus and observing the locations or timepoints of processing in the brain that are affected the most by the controlled stimulus (Hauk and Pulvermüller, 2004; Pallier et al., 2011).

More recently, researchers have begun to study the alignment of these brain language regions with the layers of language models, and found that the best alignment was achieved in the middle layers of these models (Jain and Huth, 2018; Toneva and Wehbe, 2019). This has been hypothesized to be because the middle layers may contain the most high-level language information as they are farthest from the input and output layers, which contain word-level information due to the self-supervised training objective. However, this hypothesis is difficult to reconcile with the results from more recent NLP probing tasks, which suggest that the highest-level language information should be represented by the deepest layers in the model. Taken together,

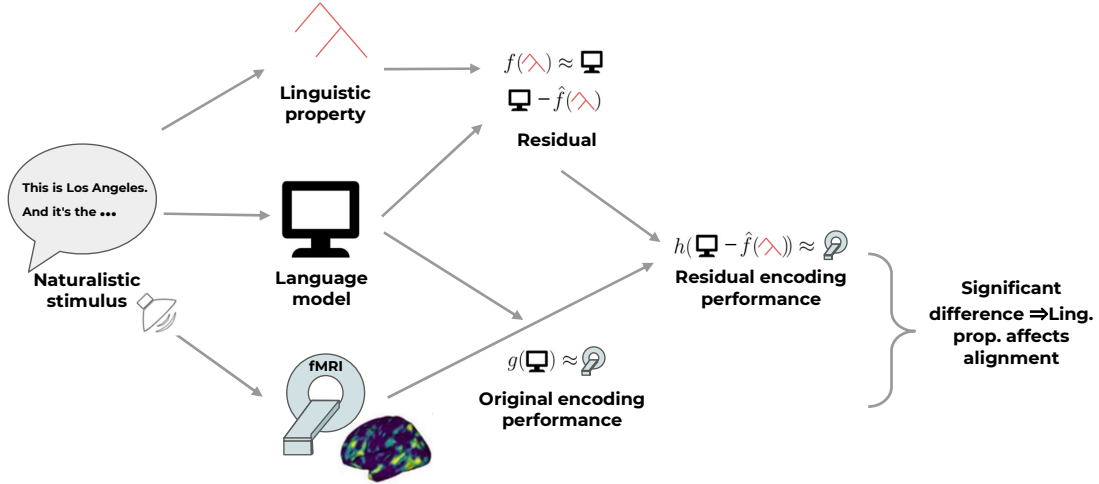


Figure 1: Approach to directly test for the effect of a linguistic property on the alignment between a language model and brain recordings. We remove the linguistic property from the language model representations and compare the brain alignment (i.e. encoding model performance) before and after the removal.

these findings leave an open question as to what linguistic information actually underlies the observed alignment between brains and language models.

Our work aims to examine this question via a direct approach (see Fig. 1 for a schematic). For a number of linguistic properties, we analyze how the alignment between brain recordings and language model representations is affected by the elimination of information related to each linguistic property. For the purposes of this work, we focus on one popular language model—BERT (Devlin et al., 2018)—which has both been studied extensively in the NLP interpretability literature (i.e. BERTology) and has been previously shown to significantly predict fMRI recordings of people processing language (Toneva and Wehbe, 2019; Schrimpf et al., 2021). We test the effect of a range of linguistic properties that have been previously shown to be represented in pretrained BERT. We use fMRI recordings that are openly available (Nastase et al., 2021) and correspond to 18 participants listening to a natural story.

Using this direct approach, we find that the elimination of each linguistic property results in a significant decrease in brain alignment across all layers of BERT. We additionally find that two of the tested linguistic properties (top constituents and word length) have the highest effect on the trend of brain alignment across model layers.

Our main contributions are as follows:

1. Propose a direct approach for evaluating the joint processing of linguistic properties in brains and language models.

2. We show that the elimination of specific linguistic properties leads to a significant decrease in brain alignment. We find that word length and top constituents are the most responsible for the trend of brain alignment across BERT layers.
3. We present a detailed study of the effect of removing linguistic properties on the alignment with specific brain regions that are thought to underlie language comprehension. Our results reveal that regions such as the bilateral AG, ATL, PTL, IFG, IFGOrb, MFG, PCC, and dmPFC experience a significant decrease in brain alignment with all layers of a pretrained language model.
4. Lastly, Tree Depth and Object Number affect the trend in alignment across layers for the ATL, MFG, IFGOrb, PCC, and dmPFC regions.

## 2 Related Work

Our work is most closely related to that of Toneva et al. (2020), who employ a similar residual approach to study the supra-word meaning of language by removing the contribution of individual words to brain alignment. We build on this approach to study the effect of specific linguistic properties on brain alignment across layers of a language model. Other recent work has examined individual attention heads in BERT and shown that their performance on syntactic tasks correlate with their brain encoding performance in several brain regions (Kumar et al., 2022). Our work presents a

complementary approach that gives direct evidence for the importance of a linguistic property to the brain alignment.

This work also relates to previous works that investigated the linguistic properties encoded across the layer hierarchy of language models (Adi et al., 2016; Hupkes et al., 2018; Conneau et al., 2018; Jawahar et al., 2019; Rogers et al., 2020). Unlike these studies in NLP, we focus on understanding the degree to which various linguistic properties impact the performance of language models in predicting brain recordings.

Our work also relates to a growing literature that relates representations of words in language models to those in the brain. A number of studies have related brain responses to word embedding methods (Pereira et al., 2016; Anderson et al., 2017; Pereira et al., 2018; Toneva and Wehbe, 2019; Hollenstein et al., 2019; Wang et al., 2020), sentence representation models (Sun et al., 2019; Toneva and Wehbe, 2019; Sun et al., 2020), recurrent neural networks (Jain and Huth, 2018; Oota et al., 2019) and Transformer methods (Gauthier and Levy, 2019; Toneva and Wehbe, 2019; Schwartz et al., 2019; Jat et al., 2020; Schrimpf et al., 2021; Goldstein et al., 2022; Oota et al., 2022; Merlin and Toneva, 2022). Our approach is complementary to these previous works and can be used to further understand the reasons behind the observed brain alignment.

### 3 Dataset Curation

**Brain Imaging Dataset** The “Narratives” collection aggregates a variety of fMRI datasets collected while human subjects listened to naturalistic spoken stories. We analyze the “Narratives-21st year” dataset (Nastase et al., 2021), which is one of the largest publicly available fMRI datasets (in terms of number of samples per participant). The dataset contains data from 18 subjects who listened to the story titled “21st year”. The dataset for each subject contains 2226 samples (TRs). The dataset was already preprocessed and projected on the surface space (“fsaverage6”). We use the multi-modal parcellation of the human cerebral cortex (Glasser Atlas: consists of 180 ROIs in each hemisphere) to display the brain maps (Glasser et al., 2016), since the Narratives dataset contains annotations that correspond to this atlas. The data covers seven language brain regions of interest (ROIs) in the human brain with the following subdivisions: (i) angular gyrus (AG: PFm, PGs, PGI, TPOJ2, and TPOJ3);

(ii) anterior temporal lobe (ATL: STSda, STSva, STGa, TE1a, TE2a, TGv, and TGD); (iii) posterior temporal lobe (PTL: A4, A5, STSdp, STSvp, PSL, STV, TPOJ1); (iv) inferior frontal gyrus (IFG: 44, 45, IFJa, IFSp); (v) middle frontal gyrus (MFG: 55b); (vi) inferior frontal gyrus orbital (IFGOrb: a47r, p47r, a9-46v), (vii) posterior cingulate cortex (PCC: 31pv, 31pd, PCV, 7m, 23, RSC); and (viii) dorsal medial prefrontal cortex (dmPFC: 9m, 10d, d32) (Baker et al., 2018; Milton et al., 2021; Desai et al., 2022).

**Extracting word features from BERT** We investigate the alignment with the base pretrained BERT model, provided by Hugging Face (Wolf et al., 2020) (12 layers, 768 dimensions). We follow previous work to extract the hidden-state representations from each layer of pretrained Transformer model: BERT (Devlin et al., 2019), given a fixed-length input length (Toneva and Wehbe, 2019). To extract the stimulus features from pretrained BERT, we constrained the tokenizer to use a maximum context of previous 20 words. Given the constrained context length, each word is successively input to the network with at most  $C$  previous tokens. For instance, given a story of  $M$  words and considering the context length of 20, while the third word’s vector is computed by inputting the network with  $(w_1, w_2, w_3)$ , the last word’s vectors  $w_M$  is computed by inputting the network with  $(w_{M-20}, \dots, w_M)$ . The pretrained Transformer model outputs token representations at different encoder layers. We use the  $\#tokens \times 768$  dimension vector obtained from the each hidden layer to obtain word-level representations from BERT.

**Downsampling** Since the rate of fMRI data acquisition (TR = 1.5sec) was lower than the rate at which the text stimulus was presented to the subjects, several words fall under the same TR in a single acquisition. Hence, we match the stimulus acquisition rate to fMRI data recording by downsampling the stimulus features using a 3-lobed Lanczos filter (LeBel et al., 2021). After downsampling, we average the word-embeddings within each TR to obtain the chunk-embedding corresponding to each TR.

**TR Alignment** To account for the slowness of the hemodynamic response, we model the hemodynamic response function using finite response filter (FIR) per voxel and for each subject separately with 8 temporal delays corresponding to 12 seconds.

**Probing Tasks** Probing tasks (Adi et al., 2016;

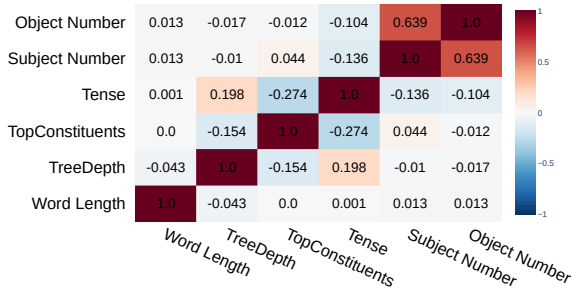


Figure 2: Task Similarity (Pearson Correlation Coefficient) constructed from the task-wise labels across six tasks.

Hupkes et al., 2018; Jawahar et al., 2019) help in unpacking the linguistic features possibly encoded in neural language models. In this paper, we use six popular probing tasks such as surface (word length), syntactic (tree depth and top constituents), and semantic (tense, subject number, and object number) to assess the capability of BERT layers in encoding each linguistic property. Since other popular probing tasks such as Bigram Shift, Odd-Man-Out, and Coordination Inversion (as discussed in (Conneau et al., 2018)) have constant labels for our brain dataset, we mainly focused on six of the probing tasks mentioned above. Details of each probing task are as follows. **Word Length:** This surface task tests for the length of a word. **TreeDepth:** This syntactic task tests for classification where the goal is to predict depth of the sentence’s syntactic tree (with values ranging from 5 to 12). **TopConstituents:** This syntactic task tests for the sequence of top-level constituents in the syntactic tree. This is a 20-class classification task (e.g. ADVP\_NP\_NP\_, CC\_ADVP\_NP\_VP\_). **Tense:** This semantic task tests for the binary classification, based on whether the main verb of the sentence is marked as being in the present (PRES class) or past (PAST class) tense. **Subject Number:** This semantic task tests for the binary classification focusing on the number of the subject of the main clause of a sentence. The classes are NN (singular) and NNS (plural or mass: “colors”, “waves”, etc). **Object Number:** This semantic task tests for the binary classification focusing on the object number in the main clause of a sentence. More details of these tasks are mentioned in (Conneau et al., 2018).

**Probing Task Annotations** To annotate the linguistic property labels for each probing task for our dataset, we use Stanford core-NLP stanza library (Manning et al., 2014) for sentence-level an-

notations. Further, for word-level annotations, we assign the same label for all the words present in a sentence except for the WordLength task.

**Probing Tasks Similarity** Pearson correlation values between task labels for each pair of tasks were used to construct the similarity matrix with heatmap for the “21st year”, as shown in Fig. 2. We observe that the following task pairs are highly correlated: (SubjNum and ObjNum), (TreeDepth and Tense), as similar to (Sileo and Moens, 2021).

## 4 Methodology

**Removal of Linguistic Properties** To remove a linguistic property from pretrained BERT representations, we use a ridge regression method in which the probing task label is considered as input and the word features are the target. We compute the residuals by subtracting the predicted feature representations from the actual features resulting in the (linear) removal of a linguistic property from pretrained features (see Fig. 1 for a schematic). Because the brain prediction method is also a linear function (see next paragraph), this linear removal limits the contribution of the linguistic property to the eventual brain prediction performance.

Specifically, given an input matrix  $\mathbf{T}_i$  with dimension  $N \times 1$  for probing task  $i$ , and target word representations  $\mathbf{W} \in \mathbb{R}^{N \times d}$ , where  $N$  denotes the number of words (8267) and  $d$  denotes the dimensionality of each word (768 dimension), the ridge regression objective function is  $f(\mathbf{T}_i) = \min_{\theta_i} \|\mathbf{W} - \mathbf{T}_i \theta_i\|_F^2 + \lambda \|\theta_i\|_F^2$  where  $\theta_i$  denotes the learned weight coefficient for embedding dimension  $d$  for the input task  $i$ ,  $\|\cdot\|_F$  denotes the Frobenius norm, and  $\lambda > 0$  is a tunable hyperparameter representing the regularization weight for each feature dimension. Using the learned weight coefficients, we compute the residuals as follows:  $r(\mathbf{T}_i) = \mathbf{W} - \mathbf{T}_i \theta_i$ .

**Voxelwise Encoding Model** To explore how linguistic properties are encoded in the brain when listening to stories, we use layerwise pretrained BERT features as well as residuals by removing each linguistic property and use them in a voxelwise encoding model to predict brain responses. If a linguistic property is a good predictor of a specific brain region, information about that property is likely encoded in that region. In this paper, we train fMRI encoding models using Banded ridge regression (Tikhonov et al., 1977) on stimuli representations from various feature spaces

Table 1: Probing task performance for each BERT layer before and after removal of each linguistic property using the 21<sup>st</sup> year stimuli.

Layers	Word Length 5-classes (Surface)		TreeDepth 8-classes (Syntactic)		TopConstituents 20-classes (Syntactic)		Tense 2-classes (Semantic)		Subject Number 2-classes (Semantic)		Object Number 2-classes (Semantic)	
	before	after	before	after	before	after	before	after	before	after	before	after
1	32.14	03.40	32.41	13.20	42.13	20.71	70.53	53.51	86.16	41.80	88.39	53.94
2	30.80	14.48	32.73	15.56	52.05	30.35	68.30	56.50	88.39	54.37	85.50	58.17
3	31.69	17.14	32.19	15.51	54.41	31.69	70.08	56.28	87.94	52.51	84.82	61.07
4	38.83	14.72	30.05	07.73	57.01	22.34	69.64	58.07	89.41	48.50	88.16	50.71
5	<b>39.73</b>	10.82	32.73	12.15	69.55	20.55	<b>74.10</b>	60.07	90.62	52.07	89.28	50.16
6	39.19	16.54	<b>35.94</b>	18.12	69.94	23.58	71.43	53.56	90.17	48.33	<b>90.17</b>	55.16
7	38.39	11.94	34.01	17.34	<b>80.04</b>	27.12	72.32	59.30	89.28	36.91	88.39	60.71
8	37.05	03.52	31.55	09.16	79.13	26.03	73.21	58.28	89.73	45.50	87.05	57.71
9	33.92	01.70	31.55	07.27	72.62	26.11	71.42	56.26	<b>91.51</b>	54.31	88.83	56.96
10	32.58	09.48	31.55	12.67	70.41	29.04	73.21	60.85	91.07	53.05	88.39	55.83
11	36.16	12.04	32.62	08.03	67.12	28.07	71.87	56.50	88.93	56.26	86.60	54.73
12	33.03	10.01	29.41	14.13	60.05	24.62	73.21	58.96	87.94	53.50	84.82	53.82

mentioned above. Before doing regression, we first z-scored each feature channel separately for training and testing. This was done to match the features to the fMRI responses, which were also z-scored for training and testing. The solution to the banded regression approach is given by  $f(\hat{\beta}) = \underset{\beta}{\operatorname{argmin}} \|\mathbf{Y} - \mathbf{X}\beta\|_F^2 + \lambda \|\beta\|_F^2$ , where  $\mathbf{Y}$  denotes the voxels matrix across TRs,  $\beta$  denotes the learned regression coefficients, and  $\mathbf{X}$  denotes stimulus or residual representations. To find the optimal regularization parameter for each feature space, we use different range of regularization parameters that is explored using five cross-validation runs. The main goal of each fMRI encoder model is to predict brain responses associated with each brain voxel given a stimuli.

**Cross-Validation** We follow 4-fold (K=4) cross-validation. All the data samples from K-1 folds were used for training, and the model was tested on samples of the left-out fold.

**Evaluation Metrics** We evaluate our models using Pearson Correlation (PC) which is a popular brain encoding evaluation metric. Let TR be the number of time repetitions. Let  $Y = \{Y_i\}_{i=1}^{TR}$  and  $\hat{Y} = \{\hat{Y}_i\}_{i=1}^{TR}$  denote the actual and predicted value vectors for a single voxel. Thus,  $Y \in R^{TR}$  and also  $\hat{Y} \in R^{TR}$ . We use Pearson Correlation (PC) which is computed as  $\operatorname{corr}(Y, \hat{Y})$  where  $\operatorname{corr}$  is the correlation function.

**Implementation Details for Reproducibility** All experiments were conducted on a machine with 1 NVIDIA GEFORCE-GTX GPU with 16GB GPU RAM. We used banded ridge-regression with following parameters: MSE loss function, and L2-decay ( $\lambda$ ) varied from  $10^{-1}$  to  $10^{-3}$ ; best  $\lambda$  was chosen by tuning on validation data; number of cross-validation runs was 5.

## 5 Results

### 5.1 Successful removal of linguistic properties from pretrained BERT

To assess the degree to which different layers of pretrained BERT representation encode labels for each probing task, a probing classifier is trained over it with the embeddings of each layer. For all probing tasks, we use logistic regression as the probe classifier. We train different logistic regression classifiers per layer of BERT using six probing sentence-level datasets created by [Conneau et al. \(2018\)](#). At test time, for each sample from 21<sup>st</sup> year, we extract stimuli representations from each layer of BERT, and perform classification for each of the six probing tasks using the learned logistic regression models. To investigate whether a linguistic property was successfully removed from the pretrained representations, we further test whether we can decode the task labels from the *residuals* for each probing task of the 21<sup>st</sup> year stimuli.

Table 1 reports the result for each probing task, before and after removal of the linguistic property from pretrained BERT. Similarly to earlier works ([Jawahar et al., 2019](#)), we find that BERT embeds a rich hierarchy of linguistic signals also for our 21<sup>st</sup> year stimuli: surface information at the initial to middle layers, syntactic information in the middle, semantic information at the middle to top layers. We verify that the removal of linguistic property of BERT leads to a reduced task performance across all layers, as expected.

### 5.2 Removal of linguistic properties significantly decreases brain alignment across all layers

In Figure 3 (left), we present the average brain alignment across all layers of pretrained BERT before and after the removal of linguistic properties

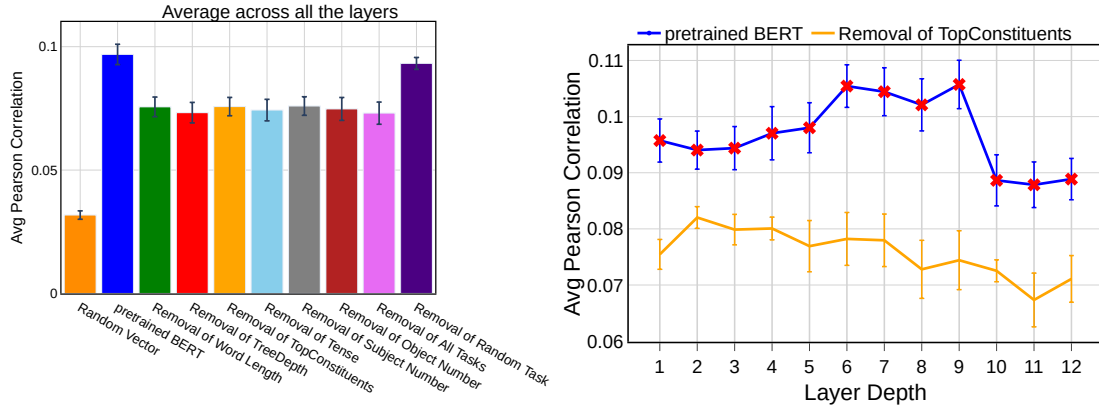


Figure 3: Brain alignment of pretrained BERT before and after removal of different linguistic properties. Left plot compares the average Pearson correlation across all layers of pretrained BERT and all voxels, and the same quantity after removal of each linguistic property. The error bars indicate the standard error of the mean across participants. The right plot compares the layer-wise performance of pretrained BERT and removal of one linguistic property—Top Constituents. A red dot at a particular layer indicates that the alignment from the pretrained model is significantly reduced by the removal of this linguistic property at this particular layer. The layer-wise results for removing other linguistic properties differ across properties, but are significant at the same layers as Top Constituents and are presented in Appendix Figure 5.

(one at a time). In comparison to the removal of each linguistic property, pretrained BERT leads to significantly better performance from intermediate to higher layers. We also validate the removal method by removing a randomly generated linguistic property vector and observe that, as expected, it does not significantly affect the alignment with the brain recordings. Further, performing the same analysis using a random vector yields lower Pearson correlation (0.03), which suggests that the linguistic properties residuals still result in better than chance performance. This result suggests that there are additional properties that are important for the alignment between pretrained BERT and the fMRI recordings, over the ones we have considered in this work.

In Figure 3 (right), we also report the layer-wise performance for pretrained BERT before and after the removal of one representative linguistic property—Top Constituents. We present the results for the remaining properties in Appendix Figure 5. Similarly to previous work (Toneva and Wehbe, 2019), we observe that pretrained BERT has best brain alignment in the middle layers. We further observe that the alignment after removing the linguistic property is significantly worse mainly for middle to late layers. Note that the layers at which there is a significant difference are indicated with a red dot. This pattern holds across all of the linguistic properties that we tested. These results provide direct evidence that these linguistic properties in fact significantly affect the alignment between

fMRI recordings and pretrained BERT.

**Statistical Significance** In order to estimate the statistical significance of the performance differences (across all tasks), we performed two-tailed paired-samples t-tests on the mean correlation values for the subjects. In all such cases, we report p-values across layers. For all layers, the main effect of the two-tailed test was significant for all the tasks with  $p \leq 0.05$  with confidence 95%. Finally, the Benjamini-Hochberg False Discovery Rate (FDR) correction (Benjamini and Hochberg, 1995) is used for all tests (appropriate because fMRI data is considered to have positive dependence (Genovese, 2000)). The correction is performed by grouping all the subject-level p-values (i.e., across removal of each linguistic property and pretrained BERT) and choosing one threshold for all of our results. Overall, the p-values confirmed that BERT is significantly better before than after the removal of the linguistic properties.

Figure 5 in the Appendix displays p-values for the brain alignment of pretrained BERT before and after the removal of each linguistic property across all the layers. We observe that the alignment with the whole brain is significantly reduced across all the layers.

**ROI-level analysis.** We further examine the effect on the alignment specifically in a set of regions of interest (ROI) that are thought to underlie language comprehension (Fedorenko et al., 2010; Fedorenko and Thompson-Schill, 2014) and word

Table 2: Correlation across layers (i) between performance of decoding task predictivity vs Brain Predictivity using Pretrained BERT, and (ii) between Brain recordings of Pretrained BERT vs Brain recordings of Residuals.

Tasks	Decoding Task with pretrained BERT vs Brain Recordings with pretrained BERT	Brain Recordings (BERT vs Residuals)
Word Length	0.571	0.182
TreeDepth	0.299	0.491
TopConstituents	0.884	0.407
Tense	0.377	0.606
Subject Number	0.681	0.589
Object Number	0.449	0.359

semantics (Binder et al., 2009). We find that across language regions, the alignment is significantly decreased by the removal of the linguistic properties across all layers, as shown in the Appendix Figure 6. We further investigate the language sub-regions, such as 44, 45, IFJa, IFSp, STGa, STSdp, STSda, A5, PSL, and STV and find that they also align significantly worse after the removal of the linguistic properties from pretrained BERT (see Appendix Figure 7).

### 5.3 Performance of decoding task prediction vs performance at predicting brain recordings

While the previous analyses revealed the importance of the linguistic properties for brain alignment at individual layers, we would also like to understand the contribution of each linguistic property to the trend of brain alignment across layers. For this purpose, we include two additional analyses: A) correlation across layers between brain alignment before removal of a linguistic property and this property’s decoding accuracy, and B) correlation across layers between brain alignment before and after the removal of a linguistic task. We present the results for these analyses for the whole brain, language regions and language sub-regions in Tables 2, 3, and 4, respectively.

**Whole brain analysis.** We make the following observations from Table 2. (1) Column A: If a pretrained BERT layer has high decoding task predictivity, it also has high brain predictivity and vice versa across all layers. High correlation values in column A show that the NLP tasks like TopConstituents, Subject Number and Word Length have a strong linear relationship with brain activations. (2) Columns A and B: If the values are high in column B but low in A, this implies that variation of brain activity prediction performance across layers is similar with or without removal of task, and brain activity prediction performance

across layers is very different from decoding task performance. This in turn implies that such tasks with high values in Column B but low in Column A (tree depth, tense) are not responsible for the bump in brain alignment in intermediate layers. On the other hand, tasks with much lower values in Column B and higher in A (like Word length, top constituents) can be considered to be responsible for the trend in brain alignment across layers. Object number and subject number marginally influence the trend in brain alignment across layers. We present the voxel-wise values of these metrics in Figure 4.

**ROI-level analysis.** Further, we analyze these correlations for each language brain region separately. For each language brain region, we report the results in Table 3. We make the following observations from Table 3: (1) TopConstituents is responsible for the bump in brain alignment not just for the entire brain but also for individual language brain areas. (2) Word Length affects the trend in alignment across layers for all brain regions except for IFG. (3) Although TreeDepth and ObjNum are not shown to be responsible for the bump in brain alignment at the whole-brain level, they affect the alignment shape more specifically for the ATL, MFG, IFGOrb, PCC, and dmPFC regions. This hypothesis aligns with previous work that has found the frontal regions to be sensitive to syntax (Friederici et al., 2003; Friederici, 2012). This implies that removal of surface (Word Length), syntactic (TreeDepth and TopConstituents) and semantic (Object Number) properties leads to significant decrease in alignment with the AG, IFGOrb, and MFG regions.

**Sub-ROI-level analysis.** We further demonstrate these correlations for each language brain sub-region separately. For each language brain sub-region, as reported in Table 4 and Appendix Table 5. We make the following observations from Table 4: (1) TopConstituents strongly affects the trend in the brain alignment across layers for individual language brain sub-regions except for IFJa. It is possible that other factors affect the trend in alignment with IFJa across layers, as this region is involved in many cognitive processes, including working memory for maintaining and updating ongoing information (Rainer et al., 1998; Zanto et al., 2011; Gazzaley and Nobre, 2012). (2) Word Length affects the trend of alignment across layers for sub-regions such as STGa, STSda, 44, 45,

Table 3: Correlation across layers for each language brain region between the brain alignment of pretrained BERT and (A) the linguistic property decoding performance of pretrained BERT, (B) brain alignment of residual BERT.

Tasks	AG		ATL		PTL		IFG		IFGOrb		MFG		PCC		dmPFC	
	A	B	A	B	A	B	A	B	A	B	A	B	A	B	A	B
Word Length	0.591	0.403	0.544	0.288	0.554	0.541	0.452	0.635	0.551	0.242	0.465	-0.029	0.653	0.076	0.343	0.091
TreeDepth	0.409	0.399	0.464	0.364	0.445	0.529	0.403	0.629	0.464	0.282	0.379	0.130	0.392	0.238	0.395	0.136
TopConstituents	0.704	0.323	0.694	0.175	0.683	0.325	0.670	0.590	0.553	0.072	0.395	-0.229	0.638	-0.160	0.545	-0.188
Tense	0.242	0.566	0.238	0.510	0.201	0.680	0.233	0.762	0.161	0.547	0.014	0.047	0.242	0.265	0.036	0.162
Subject Number	0.556	0.670	0.542	0.642	0.575	0.696	0.542	0.734	0.373	0.642	0.361	0.542	0.494	0.537	0.448	0.550
Object Number	0.624	0.669	0.582	0.485	0.652	0.759	0.593	0.847	0.646	0.519	0.595	0.199	0.611	0.251	0.464	0.188

Table 4: Correlation across layers for each language brain sub-region between the brain alignment of pretrained BERT and (A) the linguistic property decoding performance of pretrained BERT, (B) brain alignment of residual BERT.

Tasks	STGa		STSda		STSdp		44		45		IFJa		A5		TPOJ1		IFSp	
	A	B	A	B	A	B	A	B	A	B	A	B	A	B	A	B	A	B
Word Length	0.462	0.258	0.615	0.581	0.602	0.638	0.488	0.449	0.544	0.449	0.360	0.832	0.557	0.632	0.519	0.559	0.437	0.391
TreeDepth	0.472	0.311	0.405	0.679	0.452	0.634	0.437	0.621	0.532	0.621	0.306	0.829	0.388	0.628	0.457	0.529	0.277	0.312
TopConstituents	0.677	0.272	0.723	0.451	0.692	0.386	0.673	0.185	0.439	0.185	0.700	0.842	0.707	0.375	0.653	0.419	0.729	0.121
Tense	0.195	0.653	0.313	0.716	0.208	0.733	0.149	0.583	0.043	0.583	0.390	0.800	0.259	0.667	0.181	0.728	0.348	0.608
Subject Number	0.472	0.642	0.597	0.776	0.590	0.763	0.523	0.659	0.403	0.659	0.524	0.803	0.586	0.713	0.568	0.757	0.602	0.591
Object Number	0.489	0.548	0.602	0.737	0.647	0.806	0.494	0.739	0.629	0.739	0.557	0.922	0.608	0.790	0.679	0.821	0.543	0.588

and IFSp, PFm, PGI, STV and SFL. This implies that Word Length property is important in at least one sub-region of each language ROI. (3) We do not find TreeDepth and ObjNum to be important for the trend of alignment across layers with most language sub-regions except for STGa, STV, SFL, PFm, PGI and PGs. This implies that TreeDepth and all three semantic properties are not responsible for the trend in brain alignment across layers for many language sub-regions. These results suggest that there are additional properties that are important for the trend in alignment across layers between pretrained BERT and the fMRI recordings in those language sub-regions, over the ones considered in this work.

## 6 Discussion and Conclusion

We propose a direct approach for evaluating the joint processing of linguistic properties in brains and language models. We show that the removal of a range of linguistic properties from pretrained BERT leads to a significant decrease in brain alignment across all layers in the language model.

To understand the contribution of each linguistic property to the trend of brain alignment across layers, we leverage two additional analyses for the whole brain, language regions and language sub-regions: (A) correlations across layers between the performance of decoding task predictivity and brain alignment of pretrained BERT, and (B) correlations across layers between the brain alignment of pretrained BERT and the brain alignment of the residuals. For the whole brain, we find that word length and top constituents are the most responsible for the trend in brain alignment across BERT

layers. Specifically, TopConstituents is responsible for the bump in brain alignment in middle layers for all language regions whereas Word Length has impact for all brain regions except for IFG. Further, TreeDepth and ObjNum affect the trend of alignment across layers for the ATL, MFG, IFGOrb, PCC, and dmPFC regions.

One limitation of our removal approach is that any information that is correlated with the removed linguistic property in our dataset will also be removed. This limitation can be alleviated by increasing the dataset size, which is becoming increasingly possible with new releases of publicly-available datasets. It is also important to note that while we find that several linguistic properties affect the alignment between fMRI recordings and a pretrained language model, we also observed that there is substantial remaining brain alignment after removal of all linguistic properties. This suggests that our analysis has not accounted for all linguistic properties that are jointly processed. Future work can build on our approach to incorporate additional linguistic properties to fully characterize the joint processing of information between brains and language models. While we expect our conclusions to hold across multiple large language models that also encode these linguistic properties, we have only experimented with one such model here and future work should test additional models.

Overall, we hope that our approach can be used to better understand the necessary and sufficient properties that lead to significant alignment between brain recordings and language models.



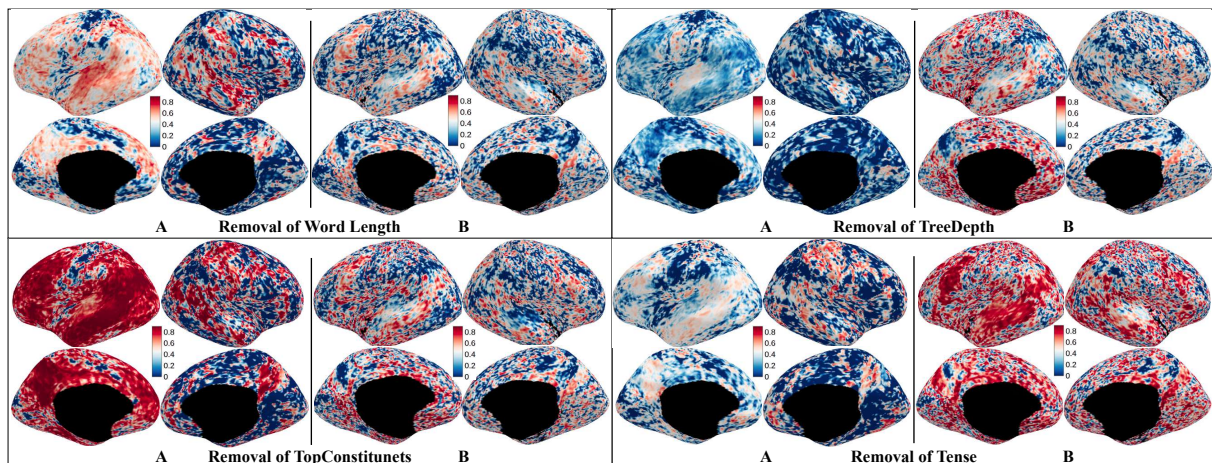


Figure 4: Voxel-wise correlations across layers between the brain alignment of pretrained BERT and (A) the linguistic property decoding performance of pretrained BERT, (B) brain alignment of residual BERT. The trend in alignment across layers for voxels with high values in column A but low values in column B is most affected by the corresponding linguistic property.

## 7 Ethical Statement

We analyse a publicly available fMRI dataset. We did not collect any new dataset.

The fMRI dataset Narratives can be downloaded from <https://datasets.datalad.org/?dir=/labs/hasson/narratives>. Please read their terms of use<sup>1</sup> for more details.

We do not foresee any harmful uses of this technology.

## References

- Yossi Adi, Einat Kermany, Yonatan Belinkov, Ofer Lavi, and Yoav Goldberg. 2016. Fine-grained analysis of sentence embeddings using auxiliary prediction tasks. *arXiv preprint arXiv:1608.04207*.
- Andrew J Anderson, Douwe Kiela, Stephen Clark, and Massimo Poesio. 2017. Visually grounded and textual semantic models differentially decode brain activity associated with concrete and abstract nouns. *TACL*, 5:17–30.
- Cordell M Baker, Joshua D Burks, Robert G Briggs, Andrew K Conner, Chad A Glenn, Kathleen N Taylor, Goksel Sali, Tressie M McCoy, James D Battiste, Daniel L O’Donoghue, et al. 2018. A connectomic atlas of the human cerebrum—chapter 7: the lateral parietal lobe. *Operative Neurosurgery*, 15(suppl\_1):S295–S349.
- Yoav Benjamini and Yoel Hochberg. 1995. Controlling the false discovery rate: a practical and powerful approach to multiple testing. *Journal of the Royal statistical society: series B (Methodological)*, 57(1):289–300.
- Jeffrey R Binder, Rutvik H Desai, William W Graves, and Lisa L Conant. 2009. Where is the semantic system? a critical review and meta-analysis of 120 functional neuroimaging studies. *Cerebral cortex*, 19(12):2767–2796.
- Charlotte Caucheteux and Jean-Rémi King. 2020. Language processing in brains and deep neural networks: computational convergence and its limits. *BioRxiv*.
- Alexis Conneau, German Kruszewski, Guillaume Lample, Loïc Barrault, and Marco Baroni. 2018. What you can cram into a single! vector: Probing sentence embeddings for linguistic properties. In *ACL 2018-56th Annual Meeting of the Association for Computational Linguistics*, volume 1, pages 2126–2136. Association for Computational Linguistics.
- Rutvik Desai, Usha Tadimeti, and Nicholas Ricciardi. 2022. Proper and common names in the semantic system.
- Jacob Devlin, Ming-Wei Chang, Kenton Lee, and Kristina Toutanova. 2018. Bert: Pre-training of deep bidirectional transformers for language understanding. *arXiv preprint arXiv:1810.04805*.
- Jacob Devlin, Ming-Wei Chang, Kenton Lee, and Kristina Toutanova. 2019. Bert: Pre-training of deep bidirectional transformers for language understanding. In *Proceedings of the 2019 Conference of the North American Chapter of the Association for Computational Linguistics: Human Language Technologies, Volume 1 (Long and Short Papers)*, pages 4171–4186.
- E. Fedorenko, P.-J. Hsieh, A. Nieto-Castanon, S. Whitfield-Gabrieli, and N. Kanwisher. 2010. New method for fMRI investigations of language: Defining ROIs functionally in individual subjects. *Journal of Neurophysiology*, 104(2):1177–1194.

<sup>1</sup><https://datasets.datalad.org/labs/hasson/narratives/stimuli/README>

- Evelina Fedorenko and Sharon L Thompson-Schill. 2014. Reworking the language network. *Trends in cognitive sciences*, 18(3):120–126.
- Angela D Friederici. 2012. The cortical language circuit: from auditory perception to sentence comprehension. *Trends in cognitive sciences*, 16(5):262–268.
- Angela D Friederici, Shirley-Ann Rüschemeyer, Anja Hahne, and Christian J Fiebach. 2003. The role of left inferior frontal and superior temporal cortex in sentence comprehension: localizing syntactic and semantic processes. *Cerebral cortex*, 13(2):170–177.
- Jon Gauthier and Roger Levy. 2019. Linking artificial and human neural representations of language. *arXiv preprint arXiv:1910.01244*.
- Adam Gazzaley and Anna C Nobre. 2012. Top-down modulation: bridging selective attention and working memory. *Trends in cognitive sciences*, 16(2):129–135.
- Christopher R Genovese. 2000. A bayesian time-course model for functional magnetic resonance imaging data. *Journal of the American Statistical Association*, 95(451):691–703.
- Matthew F Glasser, Timothy S Coalson, Emma C Robinson, Carl D Hacker, John Harwell, Essa Yacoub, Kamil Ugurbil, Jesper Andersson, Christian F Beckmann, Mark Jenkinson, et al. 2016. A multi-modal parcellation of human cerebral cortex. *Nature*, 536(7615):171–178.
- Ariel Goldstein, Zaid Zada, Eliav Buchnik, Mariano Schain, Amy Price, Bobbi Aubrey, Samuel A Nastase, Amir Feder, Dotan Emanuel, Alon Cohen, et al. 2022. Shared computational principles for language processing in humans and deep language models. *Nature neuroscience*, 25(3):369–380.
- Olaf Hauk and Friedemann Pulvermüller. 2004. Effects of word length and frequency on the human event-related potential. *Clinical Neurophysiology*, 115(5):1090–1103.
- Nora Hollenstein, Antonio de la Torre, Nicolas Langer, and Ce Zhang. 2019. Cognival: A framework for cognitive word embedding evaluation. In *CoNLL*, pages 538–549.
- Diewke Hupkes, Sara Veldhoen, and Willem Zuidema. 2018. Visualisation and ‘diagnostic classifiers’ reveal how recurrent and recursive neural networks process hierarchical structure. *Journal of Artificial Intelligence Research*, 61:907–926.
- Shailee Jain and Alexander Huth. 2018. Incorporating context into language encoding models for fMRI. In *Advances in Neural Information Processing Systems*, pages 6628–6637.
- S Jat, H Tang, P Talukdar, and T Mitchel. 2020. Relating simple sentence representations in deep neural networks and the brain. In *ACL*, pages 5137–5154.
- Ganesh Jawahar, Benoît Sagot, and Djamel Seddah. 2019. What does bert learn about the structure of language? In *ACL 2019-57th Annual Meeting of the Association for Computational Linguistics*.
- Sreejan Kumar, Theodore R Sumers, Takateru Yamakoshi, Ariel Goldstein, Uri Hasson, Kenneth A Norman, Thomas L Griffiths, Robert D Hawkins, and Samuel A Nastase. 2022. Reconstructing the cascade of language processing in the brain using the internal computations of a transformer-based language model. *bioRxiv*.
- Amanda LeBel, Shailee Jain, and Alexander G Huth. 2021. Voxelwise encoding models show that cerebellar language representations are highly conceptual. *Journal of Neuroscience*, 41(50):10341–10355.
- Christopher D Manning, Mihai Surdeanu, John Bauer, Jenny Rose Finkel, Steven Bethard, and David McClosky. 2014. The stanford corenlp natural language processing toolkit. In *Proceedings of the association for computational linguistics: system demonstrations*, pages 55–60.
- Gabriele Merlin and Mariya Toneva. 2022. Language models and brain alignment: beyond word-level semantics and prediction. *arXiv preprint arXiv:2212.00596*.
- Camille K Milton, Vukshitha Dhanaraj, Isabella M Young, Hugh M Taylor, Peter J Nicholas, Robert G Briggs, Michael Y Bai, Rannulu D Fonseka, Jorge Hormovas, Yueh-Hsin Lin, et al. 2021. Parcellation-based anatomic model of the semantic network. *Brain and behavior*, 11(4):e02065.
- Samuel A Nastase, Yun-Fei Liu, Hanna Hillman, Asieh Zadbood, Liat Hasenfratz, Neggin Keshavarzian, Janice Chen, Christopher J Honey, Yaara Yeshurun, Mor Regev, et al. 2021. The “narratives” fmri dataset for evaluating models of naturalistic language comprehension. *Scientific data*, 8(1):1–22.
- Subba Reddy Oota, Jashn Arora, Veeral Agarwal, Mounika Marreddy, Manish Gupta, and Bapi Raju Surampudi. 2022. Neural language taskonomy: Which nlp tasks are the most predictive of fmri brain activity? *arXiv preprint arXiv:2205.01404*.
- Subba Reddy Oota, Vijay Rowtula, Manish Gupta, and Raju S Bapi. 2019. Stepencog: A convolutional lstm autoencoder for near-perfect fmri encoding. In *IJCNN*, pages 1–8. IEEE.
- Christophe Pallier, Anne-Dominique Devauchelle, and Stanislas Dehaene. 2011. Cortical representation of the constituent structure of sentences. *Proceedings of the National Academy of Sciences*, 108(6):2522–2527.

- Francisco Pereira, Bin Lou, Brianna Pritchett, Nancy Kanwisher, Matthew Botvinick, and Evelina Fedorenko. 2016. Decoding of generic mental representations from functional mri data using word embeddings. *bioRxiv*, page 057216.
- Francisco Pereira, Bin Lou, Brianna Pritchett, Samuel Ritter, Samuel J Gershman, Nancy Kanwisher, Matthew Botvinick, and Evelina Fedorenko. 2018. Toward a universal decoder of linguistic meaning from brain activation. *Nature communications*, 9(1):1–13.
- Gregor Rainer, Wael F Asaad, and Earl K Miller. 1998. Memory fields of neurons in the primate prefrontal cortex. *Proceedings of the National Academy of Sciences*, 95(25):15008–15013.
- Anna Rogers, Olga Kovaleva, and Anna Rumshisky. 2020. A primer in bertology: What we know about how bert works. *Transactions of the Association for Computational Linguistics*, 8:842–866.
- Martin Schrimpf, Idan Asher Blank, Greta Tuckute, Carina Kauf, Eghbal A Hosseini, Nancy Kanwisher, Joshua B Tenenbaum, and Evelina Fedorenko. 2021. The neural architecture of language: Integrative modeling converges on predictive processing. *Proceedings of the National Academy of Sciences*, 118(45).
- Dan Schwartz, Mariya Toneva, and Leila Wehbe. 2019. Inducing brain-relevant bias in natural language processing models. *Advances in neural information processing systems*, 32.
- Damien Sileo and Marie-Francine Moens. 2021. Analysis and prediction of nlp models via task embeddings. *arXiv preprint arXiv:2112.05647*.
- Jingyuan Sun, Shaonan Wang, Jiajun Zhang, and Chengqing Zong. 2019. Towards sentence-level brain decoding with distributed representations. In *AAAI*, pages 7047–7054.
- Jingyuan Sun, Shaonan Wang, Jiajun Zhang, and Chengqing Zong. 2020. Neural encoding and decoding with distributed sentence representations. *IEEE Transactions on Neural Networks and Learning Systems*, 32(2):589–603.
- Andreĭ Nikolaevich Tikhonov, Vasilij Ja Arsenin, and Vasilii Arsenin. 1977. *Solutions of ill-posed problems*. V H Winston.
- Mariya Toneva, Tom M Mitchell, and Leila Wehbe. 2020. Combining computational controls with natural text reveals new aspects of meaning composition. *bioRxiv*.
- Mariya Toneva and Leila Wehbe. 2019. Interpreting and improving natural-language processing (in machines) with natural language-processing (in the brain). *Advances in Neural Information Processing Systems*, 32.
- Shaonan Wang, Jiajun Zhang, Haiyan Wang, Nan Lin, and Chengqing Zong. 2020. Fine-grained neural decoding with distributed word representations. *Information Sciences*, 507:256–272.
- Leila Wehbe, Ashish Vaswani, Kevin Knight, and Tom Mitchell. 2014. Aligning context-based statistical models of language with brain activity during reading. In *Proceedings of the 2014 Conference on Empirical Methods in Natural Language Processing*, pages 233–243.
- Thomas Wolf, Lysandre Debut, Victor Sanh, Julien Chaumond, Clement Delangue, Anthony Moi, Pierric Cistac, Tim Rault, Rémi Louf, Morgan Funtowicz, et al. 2020. Transformers: State-of-the-art natural language processing. In *Proceedings of the 2020 conference on empirical methods in natural language processing: system demonstrations*, pages 38–45.
- Theodore P Zanto, Michael T Rubens, Arul Thangavel, and Adam Gazzaley. 2011. Causal role of the prefrontal cortex in top-down modulation of visual processing and working memory. *Nature neuroscience*, 14(5):656–661.

## A Appendix

In Figure 5, we report the layer-wise performance for pretrained BERT before and after the removal of each of the linguistic properties. Similar to previous work (Toneva and Wehbe, 2019), we observe that pretrained BERT has best brain alignment in the middle layers across all properties. We further observe that the alignment after removing the linguistic property is significantly worse mainly for middle to late layers. Note that the layers at which there is a significant difference are indicated with a red dot. This pattern holds across all of the linguistic properties that we tested. These results provide direct evidence that these linguistic properties in fact significantly (as indicated by p-values in the right bottom of Figure 5) affect the alignment between fMRI recordings and pretrained BERT.

In Table 3, we include two analyses for each language brain region separately: 1) correlation across layers between brain alignment before and after the removal of a linguistic task, and 2) correlation across layers between brain alignment before removal of a linguistic property and this property’s decoding accuracy. We make the following observations from Table 3: (1) TopConstituents is responsible for the bump in brain alignment not just for the entire brain but also for individual language brain areas. (2) Word Length has impact for all brain regions except for IFG. (3) For the entire brain alignment, although it may seem that TreeDepth and ObjNum are not responsible for the bump in brain alignment, they seem to play a role for ATL, MFG, IFGOrb, PCC, and dmPFC regions.

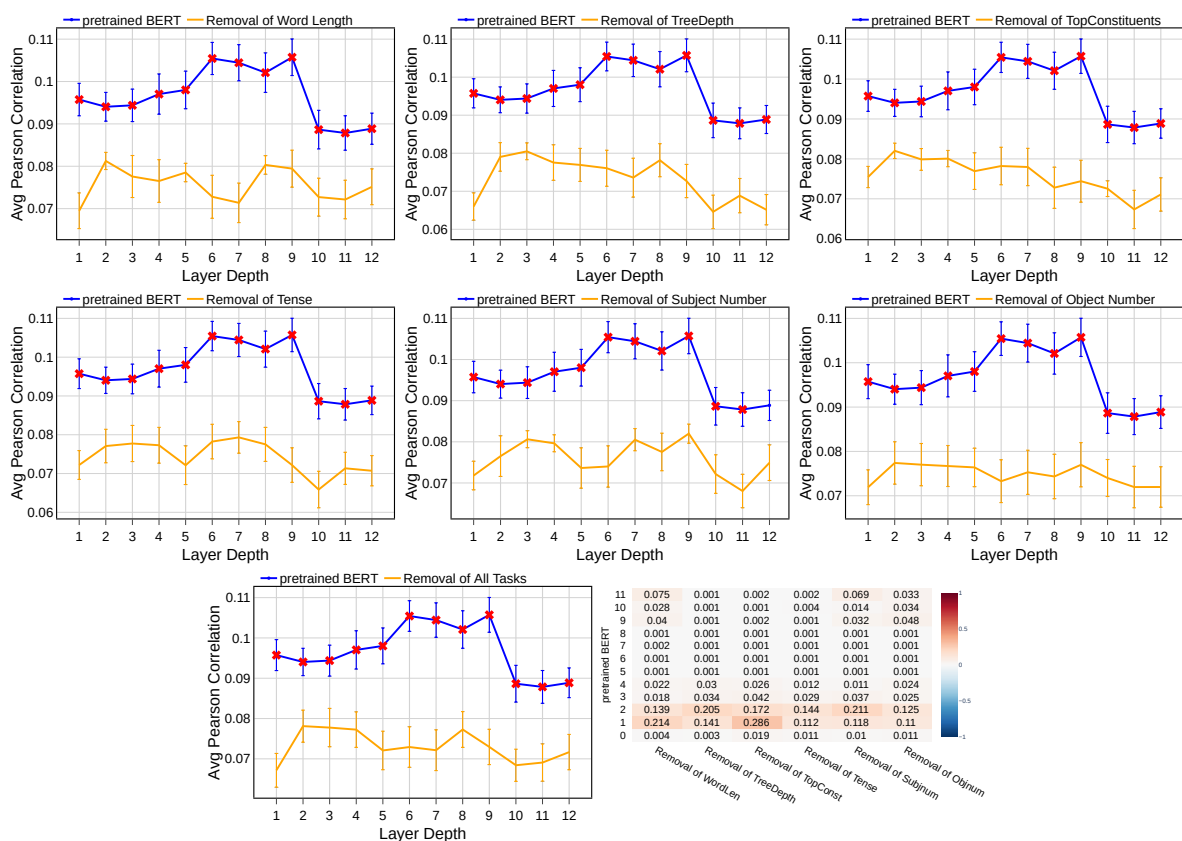


Figure 5: Model trained on pretrained BERT features and removal of different linguistic properties. Each plot compares the layer-wise performance of pretrained BERT and removal of each probing task. Bottom plot displays the pretrained BERT vs. removal of all tasks. A red dot at a particular layer indicates that the alignment from the pretrained model is significantly reduced (also indicated by p-values in the right bottom) by the removal of this linguistic property at this particular layer.

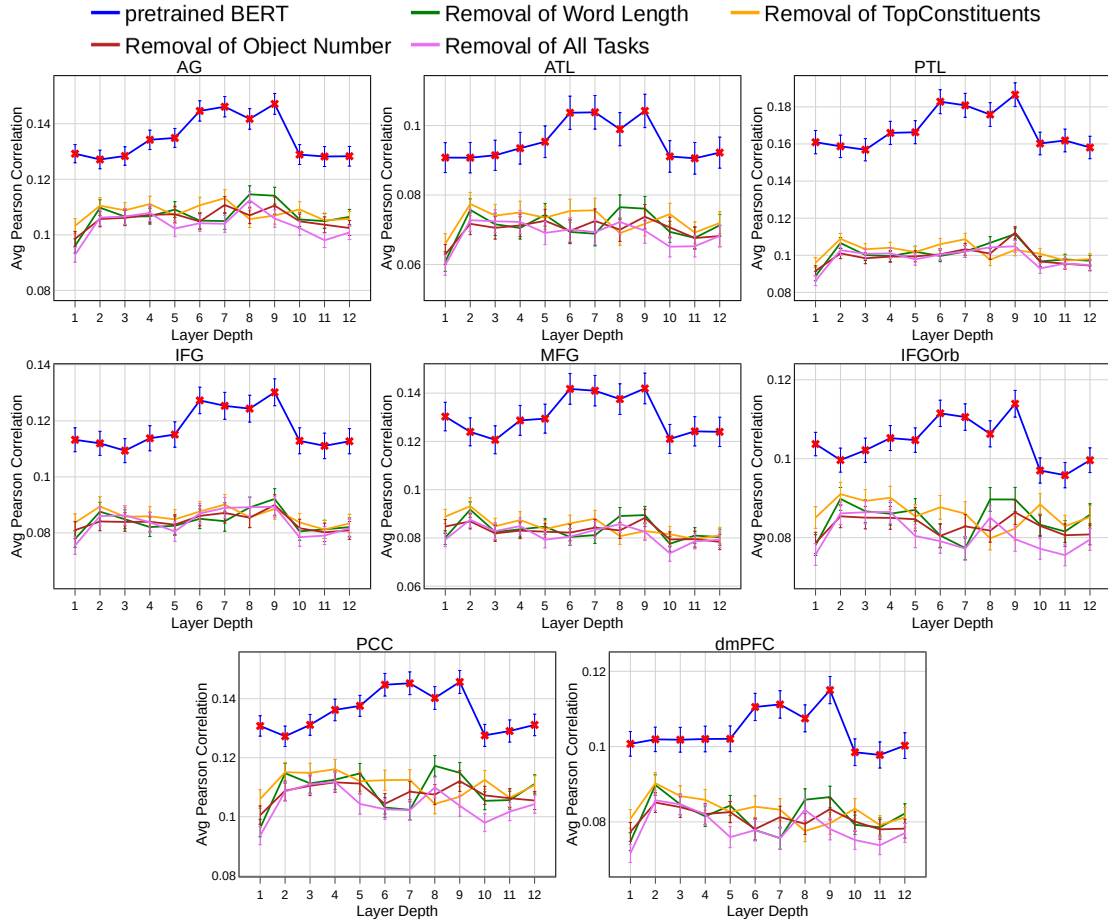


Figure 6: Avg Pearson correlations for language regions AG, ATL, PTL, IFG, MFG, IFGOrb, PCC and dmPFC. Model trained on pretrained BERT features and removal of different linguistic properties (shown only for important properties for clarity). Each plot compares the layer-wise performance of pretrained BERT and removal of each probing task.

Table 5: Correlation across layers for each language brain sub-region (A) between performance of decoding task predictivity vs Brain Predictivity using Pretrained BERT, and (B) between Brain recordings of Pretrained BERT vs Brain recordings of Residuals.

Tasks	PSL		STV		SFL		PFm		PGs		PGi	
	A	B	A	B	A	B	A	B	A	B	A	B
Word Length	0.547	0.572	0.567	0.315	0.393	0.221	0.444	0.017	0.586	0.587	0.703	0.415
TreeDepth	0.378	0.445	0.514	0.311	0.530	0.335	0.406	0.194	0.339	0.552	0.451	0.521
TopConstituents	0.704	0.338	0.550	0.362	0.385	0.137	0.357	-0.229	0.806	0.484	0.589	0.374
Tense	0.175	0.546	0.060	0.542	0.086	0.349	0.089	0.111	0.349	0.662	0.197	0.576
Subject Number	0.614	0.637	0.521	0.649	0.437	0.582	0.336	0.503	0.642	0.682	0.470	0.677
Object Number	0.637	0.708	0.702	0.546	0.635	0.341	0.564	0.287	0.563	0.677	0.709	0.687

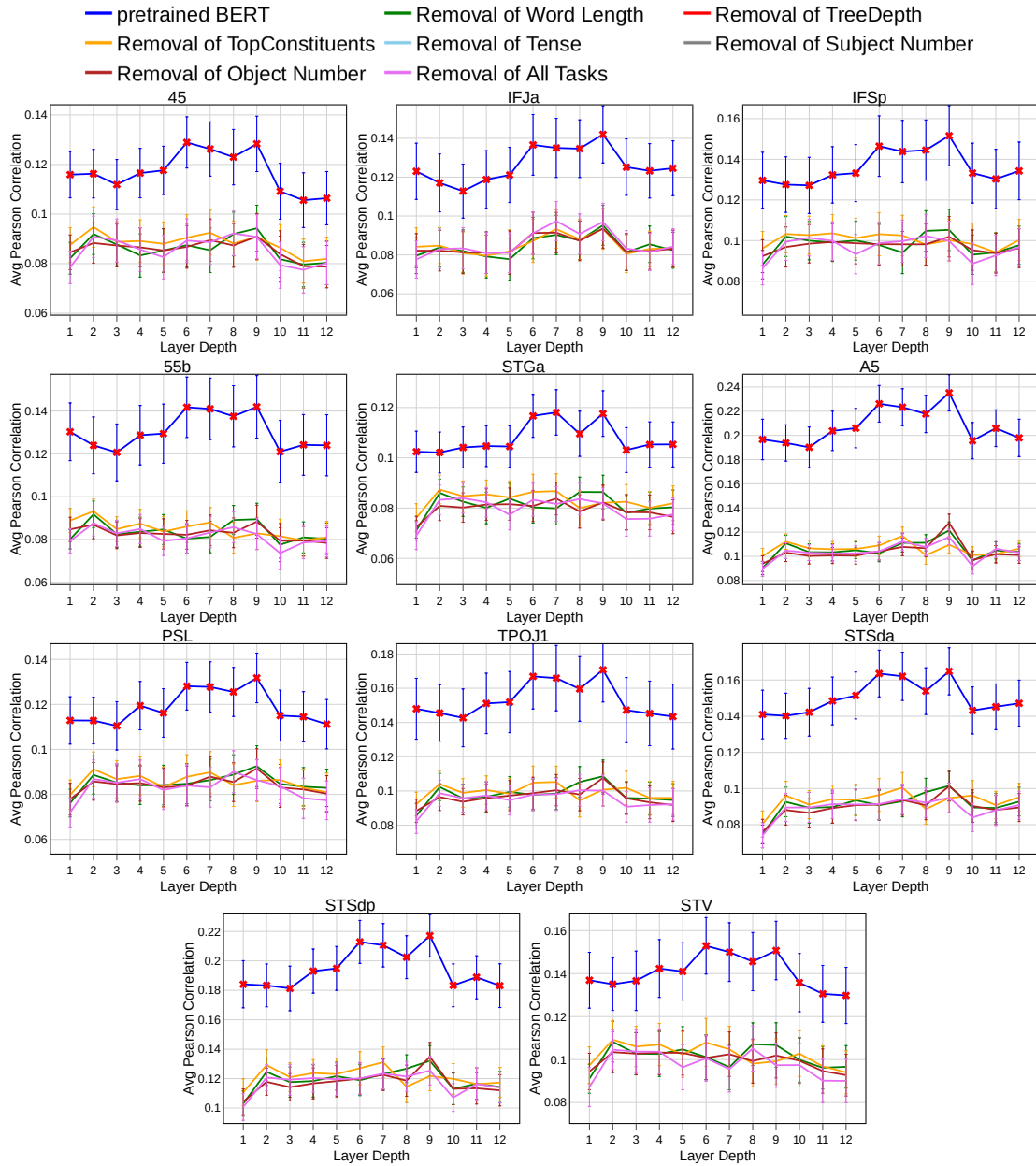


Figure 7: We extend analyses in Fig. 5 to some language sub-regions 45, IFJa, IFSp, 55b, STGa, A5, PSL, TPOJ1, STSda, STSdp and STV. Please refer to caption of Fig. 5 for detailed understanding of each plot.